COBEM 2021 Florianópolis - Brasil
26th ABCM International Congress of Mechanical Engineering
November 22-26, 2021. Florianópolis, SC, Brazil

COB-2021-0636
Physical Modeling and Parameters Identification of the MG995 Servomotor

Luiz Manoel Santos Santana
Space Robotics Laboratory (LRE), Aerospace Engineering Division - Aeronautics Institute of Technology, Praça Marechal Eduardo Gomes, 50 - Vila das Acácias, 12228-900, São José dos Campos - SP, Brazil
e-mail: luizmss@ita.br

Marcos R. O. A. Maximo
Autonomous Computational Systems Laboratory (LAB-SCA), Computer Science Division - Aeronautics Institute of Technology, Praça Marechal Eduardo Gomes, 50 - Vila das Acácias, 12228-900, São José dos Campos - SP, Brazil
e-mail: mmaximo@ita.br

Luiz Carlos Sandoval Góes
Aeronautics Systems Laboratory (LSA), Mechanical Engineering Division - Aeronautics Institute of Technology, Praça Marechal Eduardo Gomes, 50 - Vila das Acácias, 12228-900, São José dos Campos - SP, Brazil
e-mail: goes@ita.br

Abstract. *Servomotors are a very common electromechanical system. In Academy, there is a large use of Hobby servomotors, because they are low-cost while presenting a reasonable performance for education and research. However, for their use in research, there are two main issues. The first one is the absence of an encoder with position feedback. The second one is little information about the electromechanical parameters in the servomotor's datasheet. Since there is no way to obtain position feedback, an identification experiment cannot be made to obtain the servo's transfer function. The lack of information in the datasheet also hinders an attempt to obtain the transfer function from physical modeling. The main contribution of this work is a methodology to identify the transfer function and the physical parameters of a hobby servo, especially the MG995. This model was chosen due to its large popularity and low-cost. To obtain the position feedback, we needed to solder a wire on the servo's control board and decode the potentiometer's signal. This methodology can be used for other low-cost servomotors with potentiometer position feedback. After getting the position signal we made a system identification experiment to estimate the servo's transfer function. The physical parameters can be obtained by combining data from the datasheets of the MG995 servomotor and the RF-130CH DC motor, physical analyses, and the comparison between the identified transfer function and the physical modeling. To validate the methodology used to obtain the physical parameters we compare a non-linear simulation (with voltage saturation) using the estimated parameters with data collected from experimental step responses of the servo using different amplitudes. The non-linear simulation presents a behavior which closely matches with to the real data obtained from the servomotor.*

Keywords: *Servomotor, System Identification, Physical Modeling, Parameters Identification.*

1. INTRODUCTION

Servomechanisms are widely used in automation and robotics. In Academy, the use of hobby servomotors is very common. In particular, the PowerPro MG995 servomotor is widely used due to its low-cost and high torque. We can find this servo in several applications like robotic arms (Supriyono *et al.*, 2020), mobile robots (Jiko *et al.*, 2016), underwater robots (Majeed *et al.*, 2016), unmanned aerial vehicles (Chen *et al.*, 2019) and prosthetic hand (Thanakodi *et al.*, 2015). A problem found in low-cost servomotors, as is the case with the MG99, is the lack of position feedback. Position feedback is an essential element for state estimation and control systems. Position feedback is also important for obtaining the transfer function that relates the input and output of a dynamic system applying techniques of system identification. Another typical problem with low-cost servos is the little information available in their datasheet. A complete dynamic model cannot be obtained with the few parameters available. To solve the presented problems, this work has as main objectives to use a method to get the position feedback, identify the system transfer function, obtain a mathematical model that relates the angle commanded with the angle of the servo output shaft, calculate the physical parameters of the servomechanism and validate the model obtained.

The remainder of this paper is organized as follows: Section 2. shows a method to know the current position state catching a signal from servo's electronic control board; Section 3. presents a system identification experiment that obtains the MG995 transfer function; Section 4. describes how to obtain the mathematical model of the servomechanism from

physical laws; Section 5. presents the calculation of the physical parameters used in the mathematical model; Section 6. shows the results of a non-linear simulation and compare with real MG995 data to validate the model obtained in past sections; finally, Section 7. concludes the paper.

2. MEASURING THE ANGULAR POSITION SIGNAL

The goal of this section is to explain how to measure the current output shaft angle from welding a wire on the electronic control board of the servo. Subsection 2.1 describes the main elements of a typical Hobby servomotor. Subsection 2.2 details how to obtain the position signal of the potentiometer. Subsection 2.3 shows how to estimate a function that relates the voltage signal received and the current output shaft angle.

2.1 Hobby Servomotors

Servomotors are an electromechanical system widely used in engineering as an actuators for precise linear or angular motion. MG995 is a typical cheap hobby servomotor, Fig. 1 illustrates the main components of the MG995 servomotor. The DC motor converts the electrical voltage applied to its terminals in rotational motion. The gearbox decreases the speed provided by the DC motor and increases the torque applied to the output shaft. The electronic control board reads the PWM signal sent to the servo, converts it to an angle, compares it with the current angle, and calculated the control signal. Professional servomotors usually have an encoder as a position sensor. As far as we know, all servos with encoder coupled give the current position to the user. Unlike professional servomotors, the cheapest hobby servomotors typically do not have an encoder to determine the shaft position and rely on a potentiometer for this measurement. These low-cost servomotors usually have a potentiometer as an angular position sensor. The potentiometer is attached to the output shaft and rotates at the same angle as the shaft. The potetiometer's rotation along with the shaft induces a variation of the signal pin's voltage. This voltage signal is sent to the electronic control board to calculate the difference between the desired position and the current position. This error is the input of the embedded controller.

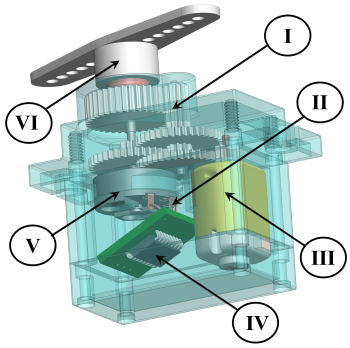

Legend	
I	Gearbox
II	Pin Signal of the Potentiometer
III	DC Motor
IV	Electronic Control Board
V	Potentiometer
VI	Output Shaft

Figure 1. Main elements of a MG995 servomotor.

2.2 Getting Potentiometer Signal

The first step to get the signal is to identify where the output pin of the potentiometer was welded on the electronic board. The output pin of the MG995 servo is the middle pin, as illustrated in Fig 2. By default, the output pin of the potentiometers is the middle pin. However, it is highly advised to test the voltage of the pins with a multimeter to validate. After discovery where is the potentiometer signal in the electronic board, a wire is soldered to this pin. Figure 3 shows a wire soldered on the electronic control board of the MG995 to get the potentiometer signal.

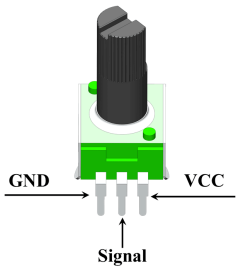

Figure 2. Potentiometer pins.

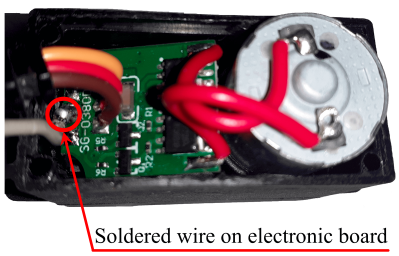

Figure 3. Place where the signal wire was soldered on electronic board.

2.3 Decoding the Signal

To decode the signal,an experiment must be done to obtain a function that relates the voltage signal of the potentiometer to the output angle. Since we observe that the shaft output angle and potentiometer signal have a linear relation, the method chosen to use is Least-Squares Method (LSM) (Ljung, 1998).

Figure 4 shows a schematic of the connections between the experiment components. The experiment components are a laptop, Arduino board, DC power supply, and the MG995 servomotor.

The power supply provides five volts to the Arduino board and the servomotor. The laptop receives the potentiometer voltage data from the Arduino and sends angles commands to the Arduino board. To do this communication between the laptop and Arduino we used the software MATLAB with the MATLAB support package for Arduino hardware (MathWorks, 2021). The Arduino sends a PWM signal relative to the desired angle and reads the voltage signal from the soldered wire on the electronic board.

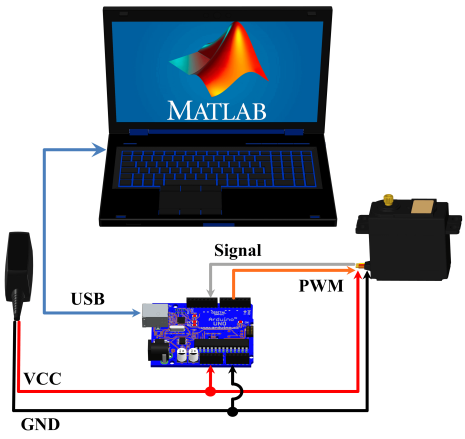

Figure 4. Default experiment setup overview.

The commanded angles vary from 0 degrees to 180 degrees by steps of 5 degrees. We wait until the servo arrive on steady state, so the angles and voltages data are organized in vectors $\vec{\boldsymbol{\theta}} = [\theta_1\ \theta_2\ \theta_3\ \ldots\ \theta_m\ ]^{\mathrm{T}}$ and $\vec{\boldsymbol{v}} = [v_1\ v_2\ v_3\ \ldots\ v_m]^{\mathrm{T}}$. Where m is the number of measurements.

The linear function that relates the voltage signal and output angle is expressed as

$$v = \alpha\theta + \beta\ , \tag{1}$$

where v is the voltage signal in volts taken from the potentiometer, θ is the output angle in degrees, and α and β are the angular and linear coefficients, respectively.

Rewriting Eq. (1) in a matrix format, considering the inputs and measures:

$$\begin{bmatrix} v_1 \\ v_2 \\ v_3 \\ \vdots \\ v_m \end{bmatrix} = \begin{bmatrix} \theta_1 & 1 \\ \theta_2 & 1 \\ \theta_3 & 1 \\ \vdots & \vdots \\ \theta_m & 1 \end{bmatrix} \begin{bmatrix} \alpha \\ \beta \end{bmatrix} \implies \vec{\boldsymbol{v}} = \boldsymbol{\Lambda} \begin{bmatrix} \alpha \\ \beta \end{bmatrix}\ . \tag{2}$$

Finally, the parameters α and β can be estimated using the LSM

$$\begin{bmatrix} \hat{\alpha} \\ \hat{\beta} \end{bmatrix} = \left[\boldsymbol{\Lambda}^{\mathrm{T}}\boldsymbol{\Lambda}\right]^{-1}\boldsymbol{\Lambda}^{\mathrm{T}}\vec{\boldsymbol{v}}\ . \tag{3}$$

For MG995 servo, the function which relates voltage signal and servo output angle is

$$v = 0.014973\,\theta + 0.297403\ . \tag{4}$$

3. SYSTEM IDENTIFICATION

This section has the purpose of presenting a system identification experiment to estimate the MG995 transfer function. This section is divided into two subsections: Subsection 3.1 shows how to obtain the transfer function, while Subsection 3.2 validates the identified transfer function.

3.1 Experiment to Identify the Transfer Function

With the data of input angle, θ_r, and output angle, θ_l, we can do an experiment to identify the transfer function that relates them. To collect the data, we used the same setup as Fig. 4. The laptop sends an angle command to the servomotor and receives the servo current position state. To do this experiment, we send a pseudorandom binary sequence (PRBS) signal to the servomotor. An ideal random signal excites the system in a large range of frequencies and, statistically, its behavior is close to a white noise signal. The PRBS was chosen because its is near a random signal. Figure 5 illustrates the PRBS signal in which the system was excited and its respective output.

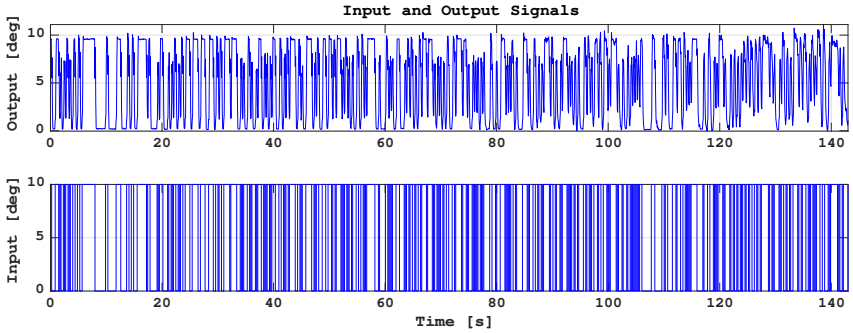

Figure 5. PRBS input and servo shaft angle.

We used the MATLAB System Identification Toolbox to execute the transfer function identification. We chose the method of instrumental variables (IV method) (Ljung, 1998). The adopted PRBS has an amplitude of 10 degrees and a sample time of 0.07 seconds (see Fig. 5). From the PRBS input and the output shaft angle calculated from Eq. (4), we estimate the following transfer function:

$$\frac{\Theta_l(s)}{\Theta_r(s)} = \frac{224.8}{s^2 + 22.33s + 225.4}. \tag{5}$$

The following pictures show the performance of the estimated transfer function compared with servo data. The plot of Fig. 6 has as input a sinusoidal function with variable amplitude and frequency. We can see that both behaviors are similar. Figure 7 shows the behavior for a step function with an amplitude of twenty degrees. Twenty degrees is twice the operating point used for the linear estimation of the transfer function. We can see that even with a considerable difference from the operating point, its behavior remained acceptable.

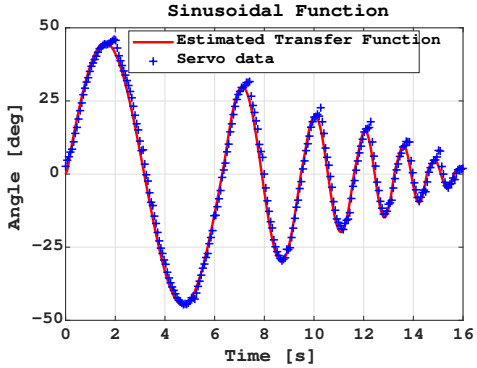

Figure 6. Servo data and transfer function simulation for a sinusoidal function with variable amplitude and frequency.

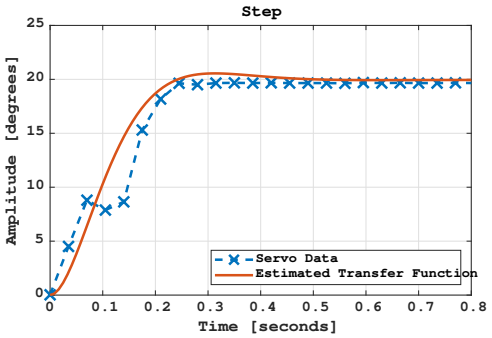

Figure 7. Servo data and transfer function simulation for a twenty degrees step response.

3.2 Transfer Function Validation

To validate the estimated transfer function, Eq.(5), we did another identification experiment using a different technique. We used the Blackman-Tukey method (Ljung, 1998). Different from the IV method, which is a parametric method, the Blackman-Tukey is non-parametric. From the Blackman-Tukey method, we obtain a spectral model of the servomotor. Therefore, we can plot a Bode diagram of the system.

The experiment is similar the one presented in subsection 3.1 We generate a PRBS signal (not the same PRBS used in subsection 3.1) with an amplitude of ten degrees. We excite the system and collect the position data. Then, we use the System Identification Toolbox from MATLAB to obtain the spectral model.

Figure 8 shows a comparison between the Bode diagram obtained from spectral analysis and the estimated transfer function. We can see that the models' behavior is similar.

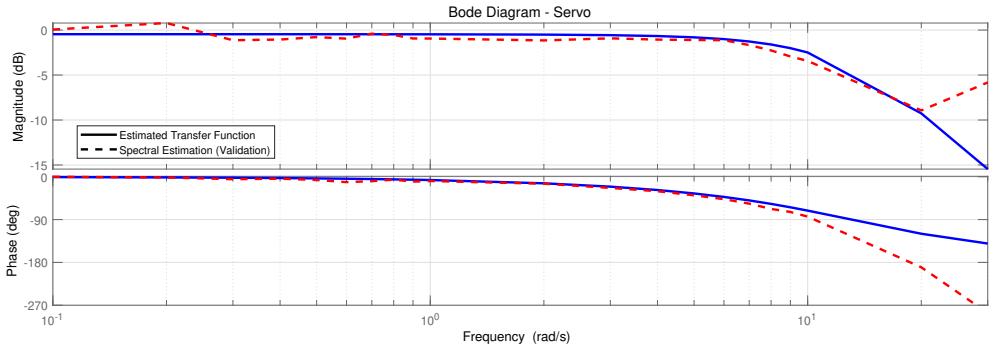

Figure 8. Bode diagram of estimated transfer function and servomotor spectral estimation.

4. PHYSICAL MODELING

In this section a mathematical model is derived based on the physical principles of the MG995 servomotors. This modeling is standard and could be used for most servomotor. Figure 9 shows the main physical parameters that define servomotor dynamics.

In the electrical dynamics shown in the diagram of Fig. 9, u is the voltage applied to the the motor terminals, i is the electrical current, R is the motor resistance, L is the inductance, and e is the back electromotive force.

Now, the mechanical elements are τ_m who is the torque produced by the motor, J_m is the motor moment of inertia, b_m is the viscous friction coefficient, τ_f is the viscous friction torque, θ_m is the angle of rotation in the motor shaft, N is the gearbox gear ratio, J_l is the moment of the inertia of the load attached to the servo output shaft, τ_l is the torque applied to the load in the output shaft and, finally, θ_l is the rotational angle of the servo output shaft.

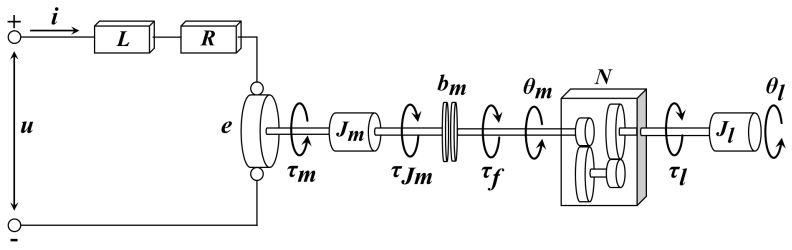

Figure 9. Dynamical elements of a servomotor.

The next two subsections, Subsection 4.1 and Subsection 4.2, are going to describe the mathematical modeling for the MG995 servomotor.

4.1 Open-Loop Mathematical Model

The objective of this subsection is to obtain a transfer function that represents the open-loop dynamics $P(s)$ of a servo motor for a voltage input $U(s)$ and as output the angle of the servo output shaft $\Theta_l(s)$. Figure 10 describes the block diagram of the open-loop system.

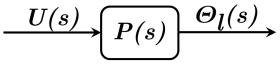

Figure 10. Open-Loop block diagram.

The main equations of motion of a standard servo may be described by the following equations [Sen (1996); Maximo *et al.* (2017)]:

$$\tau_m = K_t i \ , \tag{6}$$

$$u = Ri + L\frac{di}{dt} + e \ , \tag{7}$$

$$e = \frac{\dot{\theta}_m}{K_\omega} \ , \tag{8}$$

$$J_m\ddot{\theta}_m = \tau_m - \frac{\tau_l}{\eta N} - \tau_f \ , \tag{9}$$

$$\tau_l = J_l\ddot{\theta}_l \ , \tag{10}$$

$$K_t = K_\omega^{-1} \ , \tag{11}$$

$$\tau_f = b_m\dot{\theta}_m \ , \tag{12}$$

where K_t is the motor torque constant, K_ω is the speed constant, and η is the gearbox efficiency factor.

From Eq.(9) and Eq.(10):

$$\tau_l = J_l\ddot{\theta}_l = \eta N\left[\tau_m - \tau_f - J_m\ddot{\theta}_m\right] \ . \tag{13}$$

Using Eq.(6) and Eq.(12) in Eq.(13):

$$J_l\ddot{\theta}_l = \eta N\left[K_t i - b_m\dot{\theta}_m - J_m\ddot{\theta}_m\right] \ . \tag{14}$$

For an ideal gearbox, the conservation of power implies that the input power P_m of the gearbox is equal to the output power P_l, but in practice the output power is reduced with respect to the input power,the gearbox efficiency factor η describes this power loss:

$$P_m = P_l \implies \dot{\theta}_m = N\dot{\theta}_l \implies \ddot{\theta}_m = N\ddot{\theta}_l \ . \tag{15}$$

Applying Eq.(15) in Eq.(14):

$$J_l\ddot{\theta}_l = \eta N\left[K_t i - b_m N\dot{\theta}_l - J_m N\ddot{\theta}_l\right] \ . \tag{16}$$

Considering null initial conditions, taking the Laplace transform of Eq.(16) and doing some algebraic manipulations, we find the transfer function from current $I(s)$ to the angle $\Theta_l(s)$

$$\frac{\Theta_l(s)}{I(s)} = \frac{N\eta K_t}{\left(J_l + J_m\eta N^2\right)s^2 + \left(b_m\eta N^2\right)s} \ . \tag{17}$$

Now, merging Eq.(7), Eq.(8) and Eq.(15):

$$u = Ri + L\frac{di}{dt} + \frac{N\dot{\theta}_l}{K_\omega} \ . \tag{18}$$

Taking the Laplace transform of the Eq.(18):

$$U(s) = (R + Ls)\, I(s) + \frac{Ns}{K_\omega}\Theta_l(s) \ . \tag{19}$$

We can merge Eq.(17) and Eq.(19), do some algebraic manipulation to find the transfer function which relates the input voltage $U(s)$ and the output angle $\Theta_l(s)$ of the load shaft:

$$P(s) = \frac{\Theta_l(s)}{U(s)} = \frac{\eta N K_t}{\left\{(R + Ls)\left[\left(J_m\eta N^2 + J_l\right)s + b_m\eta N^2\right] + \eta N^2 K_t^2\right\}s} \ . \tag{20}$$

4.2 Closed-Loop Mathematical Model

Figure 11 shows the closed-loop system of the servo. We assume that the controller $C(s)$ of low-cost servomotor use a proportional control. The input of the closed-loop control is the commanded angle $\Theta_r(s)$. The feedback signal is the load output shaft angle $\Theta_l(s)$. $E(s)$ is the error, and $P(s)$ is the servo open-loop dynamics represented by Eq.(20).

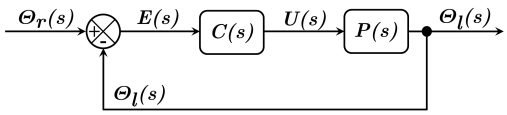

Figure 11. Closed-Loop block diagram.

For the closed-loop system, we will start from the open-loop transfer function of Eq. (20). To simplify the notation, we will adopt $J_{eq} = J_l + J_m\eta N^2$ and $b_{eq} = b_m\eta N^2$.

Assuming that MG995 use a proportional controller with gain K_P:

$$G(s) = \frac{\Theta_l(s)}{E(s)} = \frac{\eta N K_t K_P}{\left[(R + Ls)\left(J_{eq}s + b_{eq}\right) + \eta N^2 K_t^2\right] s} \,. \tag{21}$$

Doing the feedback:

$$\frac{\Theta_l(s)}{\Theta_r(s)} = \frac{G(s)}{1 + G(s)} = \frac{\eta N K_t K_P}{\left[(R + Ls)\left(J_{eq}s + b_{eq}\right) + \eta N^2 K_t^2\right] s + \eta N K_t K_P} \,. \tag{22}$$

Now, we can do some reductions. How the electrical dynamics is much faster than the mechanical one, $i.e.$, the time constant $\frac{R}{L}$ is much smaller than the mechanical time constant, we can be disregarded it (Maximo *et al.*, 2017). So, considering $L \approx 0$, the closed-loop equation which represents the servomechanism is

$$\frac{\Theta_l(s)}{\Theta_r(s)} = \frac{\eta N K_t K_P}{R J_{eq} s^2 + \left(R b_{eq} + \eta N^2 K_t^2\right) s + \eta N K_t K_P} \,. \tag{23}$$

5. PARAMETERS IDENTIFICATION

This section has the aim of determining the MG995 physical parameters. These parameters are gear ratio N (Subsection 5.1), torque constant K_t of the motor (Subsection 5.2), gearbox efficiency factor η (Subsection 5.3), viscous friction coefficient b_m (Subsection 5.4), the moment of inertia of the motor J_m (Subsection 5.5) and the proportional gain of the controller K_P (Subsection 5.6). For this, we use data from motor and servo datasheets (Mabuchi, 2021; Towerpro, 2021) , shown on Table 1, servo's characteristics, dynamics equations, and comparison with the estimated transfer function (Eq. 5). Table 1 show the know parameters. The output torque in stall operation τ_l^{Stall} was get from MG995 datasheet, were stall operation is when $\dot{\theta}_m = 0$. The motor's torque in stall operation τ_m^{Stall}, motor's current in stall operation i_m^{Stall}, motor's shaft angular velocity in no load operation $\dot{\theta}_m^{NoLoad}$ and motor's current in no load operation i_m^{NoLoad} was get from RF-130CH DC motor datasheet. Where $NoLoad$ is when there is no load in the motor shaft. The resistance $R = 2.5\ \Omega$ was measured with a multimeter. To validate the calculated parameters, in Subsection 5.7 we did an experiment using a mass attached to the servo shaft. So, we comparing the estimated transfer function obtained from the experiment with the calculated data of this section.

Parameters				
τ_l^{Stall} (Nm)	τ_m^{Stall} (Nm)	i_m^{Stall} (A)	$\dot{\theta}_m^{NoLoad}$ (rad/s)	i_m^{NoLoad} (A)
0.9218	0.00412	0.7	848.23	0.036

Table 1. Datasheet Parameters.

5.1 Gear Ratio N

There is no information about the gearbox on the servo datasheet. To know the gear ratio we opened the gearbox and counted the number of teeth of each gear. Figure 12 illustrates the schematic of the gearbox transmission, Table 2 describes the number of teeth of the gears, Figure 13 shows the opened gearbox.

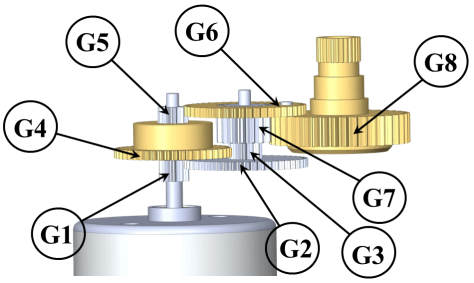

Figure 12. MG995 gearbox.

Gear	Number of Teeth
G1	12
G2	64
G3	12
G4	48
G5	12
G6	48
G7	13
G8	42

Table 2. Gearbox gears' teeth.

Figure 13. Opened gearbox.

The gear ratio N can be calculated respecting the transmission order of Figure 12 and the respective number of teeth of the gears, as described in the Table 2.

$$N = \frac{G2}{G1}\frac{G4}{G3}\frac{G6}{G5}\frac{G8}{G7} = \frac{64}{12}\frac{48}{12}\frac{48}{12}\frac{42}{13} \implies N = 275.6923\ [\ ]\ . \tag{24}$$

5.2 Torque K_t Constant

K_t can be calculated using the data of the motor datasheet and using Eq.(11).

$$K_t = \frac{\tau_m^{Stall}}{i_m^{Stall}} = 5.8857 \times 10^{-3}\ (\mathrm{Nm/A})\ . \tag{25}$$

5.3 Gearbox Efficiency Factor η

The gearbox efficiency factor η can be calculated by the torque transmission:

$$\eta = \frac{\tau_l^{Stall}}{N\tau_m^{Stall}} \implies \eta = 0.81156\ [\ ]\ . \tag{26}$$

5.4 Viscous Friction Coefficient b_m

The viscous friction coefficient can be calculated from the motor datasheet data and using Eq (12).

$$K_t i_m^{NoLoad} = b_m \dot{\theta}_m^{NoLoad} \implies b_m = \frac{K_t i_m^{NoLoad}}{\dot{\theta}_m^{NoLoad}} \implies b_m = 2.49797 \times 10^{-7}\ (\mathrm{Nms})\ . \tag{27}$$

5.5 Motor Moment of Inertia J_m

Associating the second term of the characteristic equation of the transfer function modeled from physical principles,Eq.(23), with the second term of the equation characteristic of the estimated transfer function, Eq.(5), we can calculate de moment of the motor inertia J_m.

$$\frac{1}{J_m}\left(b_m + \frac{K_t^2}{R}\right) = 22.33 \implies J_m = 6.3173 \times 10^{-7}\ \left(\mathrm{Kgm^2}\right)\ . \tag{28}$$

5.6 Controller Proportional Gain K_P

To compute the proportional gain K_P, we performed a procedure similar to the one presented previously to calculate J_m. Equating the third term of the characteristic equation of the transfer function of the Eq.(23), with the third term of the characteristic equation of the estimated transfer function Eq.(5).

$$\frac{K_t K_P}{R J_m N} = 225.4 \implies K_P = 16.6742\ [\ ]\ . \tag{29}$$

5.7 Parameters Validation

To validate the parameters obtained in Section 5., in this subsection we prepare an experiment changing the moment of inertia of the load J_l, using a load attached to the servo output shaft, how illustrated in Fig. 15. Using a cylinder with mass = 0.1 kg, radius = 0.022 m and length = 0.025 m, attached in a distance of 0.05 m from the rotation axis, we did a data collection and transfer function estimation similar to Section 3.The dynamics of this estimated transfer function are compared with the calculated transfer function, using the parameters of Tab. 3 and Eq.(23).

MG995 Parameters	
R	2.5 (Ω)
K_t	5.8857×10^{-3} (Nm/A)
K_ω	169.9029 (rad/V)
J_m	6.3173×10^{-7} (Kgm^2)
N	275.6923 [ ]
η	0.81156 [ ]
b_m	2.49797×10^{-7} (Nms)
K_P	16.6742 [ ]

Table 3. Dynamic Parameters.

Using the Steiner's theorem:

$$J_l = J_{cyl} + md^2. \tag{30}$$

Where J_{cyl} is the cylinder inertia.
Remembering that $J_{eq} = J_l + J_m \eta N^2$, the J_{eq} could be rewrite as:

$$J_{eq} = J_{cyl} + md^2 + J_m \eta N^2. \tag{31}$$

In Figure 14 there is a comparison between the dynamics of the calculated and estimated transfer function. We can see that the behavior is close.

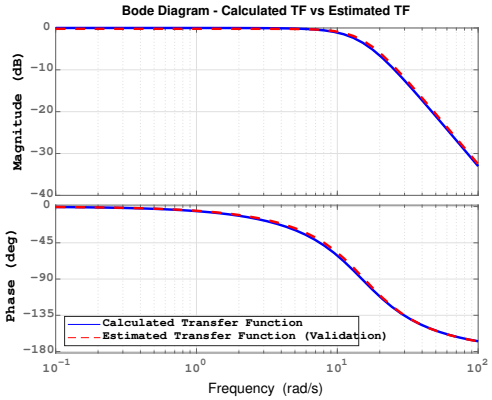

Figure 14. Comparison of the estimated and calculated transfer function dynamics.

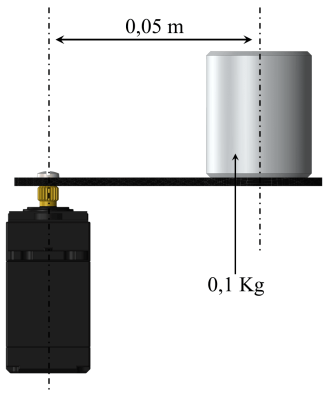

Figure 15. Experiment overview.

6. MODEL VALIDATION

In this section, we will show the results for a non-linear simulation of the found servomotor parameters, see Table 3, considering the motor's voltage saturation. Motor's voltage saturation generates a delay in the response of the system when compared to the linearized model.

We used a voltage saturation according to the maximum voltage of the power supply, $i.e.$, 5V.

Figure 16 shows the results for step responses to servo data and the non-linear model simulation. We can see that the time response os simulation matches well the real data. Therefore, the results obtained in this work are validated.

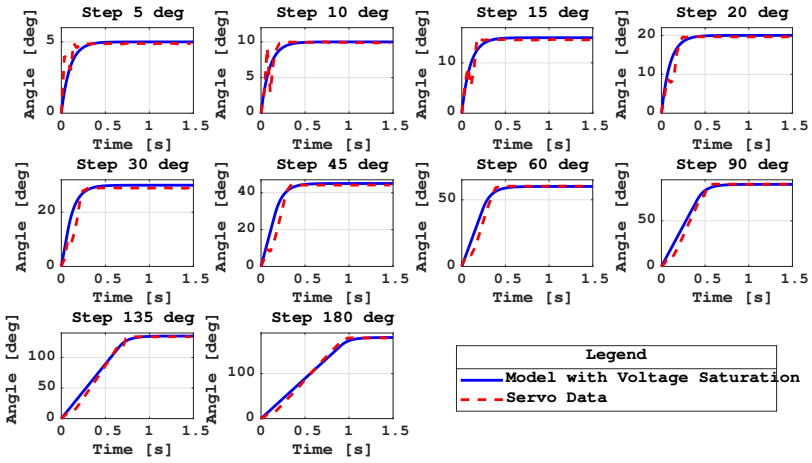

Figure 16. Results for the non-linear model.

7. CONCLUSION

This paper proposed to discover the transfer function, mathematical model, and physical parameters of the MG995 servo. Hobby servomotors usually do not have a external position feedback, thus making a system identification experiment impossible to find the transfer function. The little information in the datasheet makes it difficult to obtain the transfer function by mathematical modeling. For the problem of the lack of position feedback, we show a technique to obtaining position data from the potentiometer voltage. Using the position feedback, we did a system identification experiment to find the servo transfer function. We did the mathematical modeling of the servomechanism to be able to represent the transfer function from its physical parameters. From the data in the datasheets, dynamic equations, mechanical characteristics of the servo, and the estimated transfer function, we obtained all the necessary dynamic parameters of the servomechanism. For validation, we did a non-linear simulation, considering the voltage saturation, and compared it with real system data for several step amplitudes. The behavior of the simulation with the physical parameters was very close to the real system. The methodology used in this work can be applied to other hobby servomotors.

8. ACKNOWLEDGMENTS

The author Luiz M. S. Santana acknowledges the scholarship financial support of Coordination of Superior Level Staff Improvement - CAPES.

9. REFERENCES

Chen, Y. *et al.*, 2019. "An effective spray drift-reducing method for a plant-protection unmanned aerial vehicle". *International Journal of Agricultural and Biological Engineering*.

Jiko, M.N. *et al.*, 2016. "Design and implementation of amphibious smart rescue robot". In *2nd International Conference on Electrical, Computer & Telecommunication Engineering*.

Ljung, L., 1998. *System Identification: Theory for the User*. Pearson Education.

Mabuchi, 2021. "Rf130ch datasheet". `https://bit.ly/3wMejfG`. Accessed: 2021-06-20.

Majeed, A. *et al.*, 2016. "Design and implementation of swimming robot based on carp fish biomimetic". In *Al-Sadeq International Conference on Multidisciplinary in IT and Communication Science and Applications*.

MathWorks, 2021. "Matlab support package for arduino hardware". `https://bit.ly/3zHsVik`. Accessed: 2021-06-20.

Maximo, M.R.O.A. *et al.*, 2017. "Modeling of a position servo used in robotics applications". *Proceedings of the 2017 Simpósio Brasileiro de Automaçao Inteligente (SBAI), Porto Alegre, SC, Brazil*.

Sen, P.C., 1996. *Principles of Electric Machines and Power Electronics*. John Wiley & Sons Inc, 2nd edition.

Supriyono, W. *et al.*, 2020. "Alternative control system for robot arm with data logger". *International Journal of Advanced Trends in Computer Science and Engineering*.

Thanakodi, S. *et al.*, 2015. "Prosthetic hand controlled by wireless flex sensor on eod robot". In *International Conference for Innovation in Biomedical Engineering and Life Sciences*.

Towerpro, 2021. "Mg995 datasheet". `https://www.towerpro.com.tw/product/mg995/`. Accessed: 2021-06-20.

10. RESPONSIBILITY NOTICE

The authors are solely responsible for the printed material included in this paper.